EFFECT OF A RADIATION SHIELD ON SILICON CZ GROWTH

TAKAO TSUKADA, NOBUYUKI IMAISHI, MITSUNORI HOZAWA AND KATSUHIKO FUJINAWA
Chemical Research Institute of Non-Aqueous Solutions, Tohoku University, Sendai 980

Key Words: Crystal Growth, Silicon, Czochralski Method, Radiation Shield, Heat Conduction, Interface Shape, Numerical Simulation, Finite Element Method

For silicon CZ crystal growth, the effect of inserting a radiation shield into the furnace on the temperature profile in the melt and crystal and on the shape of the melt/crystal interface was studied theoretically by use of finite element analysis based on the conduction-dominated model.

It was found that inserting a radiation shield makes the interface shape less convex to the crystal in comparison with that without the shield except for the initial stage. Also, with use of a short radiation shield there is a possibility of obtaining a higher pull rate because the temperature gradient near the interface becomes steeper than that without the shield.

Introduction

Single crystals supplied for semiconductor devices are mostly pulled by the Czochralski (CZ) method. In crystal growth by the CZ method, the shape of the melt/crystal interface affects crystal perfection and radial distribution of dopant, while the temperature variation in the crystal produces thermal stress and leads to the generation of dislocations. Accordingly, it is important to acquire knowledge about the heat transfer mechanism in both the melt and crystal and the shape of the melt/crystal interface for various growing conditions.

Though heat transfer in the melt and the shape of the melt/crystal interface are influenced by convection in the melt, those for a system with small Prandtl number, such as silicon and germanium, can be approximated by the conduction-dominated model.

There are two theoretical methods to obtain the temperature distribution in the melt or/and crystal for CZ growth. The first method gives the temperature profile in the crystal, assuming the interface to be flat and at the melting-point temperature. Rea[9] and Hart *et al.*[6] solved the one-dimensional conduction-dominated problem and provided guidance for the operational mode of crystal growth. Williams *et al.*[12] developed the two-dimensional heat transfer model and computed the temperature profile in the growing crystal by use of the finite element method.

The second method determines the melt/crystal interface shape and the temperature fields in the melt and crystal simultaneously. Arizumi *et al.*[1,2] obtained the interface shape and the temperature distribution by solving the Laplace equation numerically by use of the finite difference method and suggested for germanium crystal growth that the interface shape was a function of convection heat loss from crystal surface, crystal length, crystal radius and crucible temperature.

Recently, Derby *et al.*[3–5] carried out a finite element analysis of the CZ and Liquid Encapsulated Czochralski crystal growth based on the thermal-capillary model. They computed the heat transfer in the melt and crystal and the shapes of melt/crystal and melt/gas interfaces for various conditions and proposed processing strategies for uniform crystal growth.

Also, Ramachandran *et al.*[8,11] simulated numerically the temperature profile and both interface shapes by use of the finite element method, accounting for both directed and reflected radiation, and investigated the effect of various process parameters on the melt/crystal interface shape and the pull rate.

However, there have been no reports which give details of the heat transfer mechanism in the melt and crystal in the case where a radiation obstacle is present.

The aim of this theoretical work is to analyze the effect of a radiation shield inserted between the crystal rod and crucible, as shown in **Fig. 1**, on the temperature distribution in the melt and crystal and the melt/crystal interface shape, by use of the thermal-capillary model.

1. Theory

Figure 1 shows the coordinate system used here. The cylindrical-shaped radiation shield is placed in the furnace.

Received July 30, 1986. Correspondence concerning this article should be addressed to T. Tsukada.

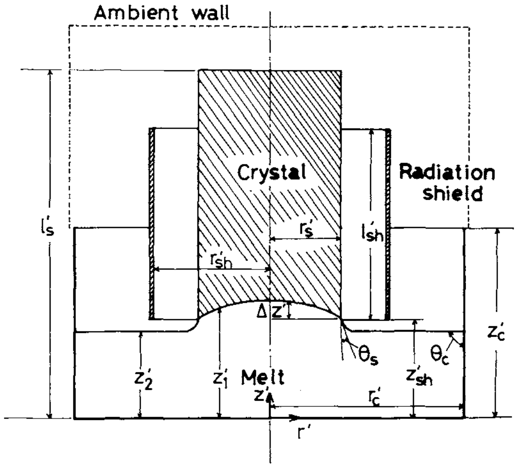

Fig. 1. Coordinate system.

The following assumptions are made in the numerical simulations. 1) The crystal is pulled continuously from the melt at a constant rate, but the system is supposed to be in a pseudo-steady state, since the pull rate is very small. 2) The system is rotationally symmetric. 3) The heat transfer within the melt, crystal and radiation shield is dominated only by conduction. 4) The crucible and the ambient temperature are constant. 5) The heat loss from each boundary surface is due only to radiation. 6) The melt/crystal interface is at the melting-point temperature. 7) The contact angles of melt against the crystal and the crucible are constant.

Under the above assumptions, the dimensionless forms of the energy equations for the melt, crystal and radiation shield are given as follows, where the length and temperature are non-dimensionalized by crucible radius r'_c and melting-point temperature T'_m respectively.

$$\nabla \cdot \nabla T_l = 0 \tag{1}$$

$$Pe\boldsymbol{e}_z \cdot \nabla T_s = \nabla \cdot \{\kappa_s(T_s)\nabla T_s\} \tag{2}$$

$$\nabla \cdot (\kappa_{sh}\nabla T_{sh}) = 0 \tag{3}$$

where suffixes l, s and sh mean the melt, crystal and radiation shield respectively, κ_s, κ_{sh} are thermal conductivity ratio to that of the melt, and Pe corresponds to the dimensionless pull rate.

The boundary conditions are expressed as follows.

At the side and bottom of the crucible:

$$T_l = T_c \tag{4-1}$$

At the melt/gas interface:

$$-\boldsymbol{n} \cdot \nabla T_l = q_{rad,l} \tag{4-2}$$

At the melt/crystal interface:

$$\boldsymbol{n} \cdot \nabla T_l - \kappa_s \boldsymbol{n} \cdot \nabla T_s = PeSt\boldsymbol{n} \cdot \boldsymbol{e}_z \tag{4-3}$$

$$T_l = T_s = 1 \tag{4-4}$$

At the side and top of the crystal:

$$-\kappa_s \boldsymbol{n} \cdot \nabla T_s = \dot{q}_{rad,s} \tag{4-5}$$

At the inside, outside, bottom and top of the radiation shield:

$$-\kappa_{sh}\boldsymbol{n} \cdot \nabla T_{sh} = q_{rad,sh} \tag{4-6}$$

At the center line:

$$\boldsymbol{n} \cdot \nabla T_l = \boldsymbol{n} \cdot \nabla T_s = 0 \tag{4-7}$$

In the above equations, $q_{rad,k}(k = l, s \text{ and } sh)$ is heat loss per unit area on the boundary surface due to radiation, taking both directed and reflected radiation heat exchange between individual surface element and all surrounding surfaces into account. $q_{rad,k}$ on the surface element at temperature T_k is described as follows, by use of the enclosure analysis method by Gebhart.[10)]

$$q_{rad,k} = (R_l/\varepsilon_l)\left\{\varepsilon_k(T_k)T_k^4 - \left(\sum_{j=1}^{N} A_j\varepsilon_j T_j^4 G_{jk}\right)\Big/A_k\right\} \tag{5}$$

where R_l is radiation number, N is total number of radiation surface elements present and G_{jk} is Gebhart's absorption factor, which is the fraction of the emission from surface A_j that reaches A_k and is absorbed. In calculation of G_{jk} in Eq. (5), a configuration factor F_{jk} is required. F_{jk} is obtained by numerical integration since the radiation shield makes the geometrical configuration complicated and makes the analytical solution[8,11)] of F_{jk} quite cumbersome.

Accordingly, the temperature fields in the melt, crystal and radiation shield are given by solving Eqs. (1)–(3) under the boundary conditions.

The melt/crystal interface shape z_1 is determined such that Eq. (4-4), where the interface is at the melting-point isotherm, is satisfied.

The melt/gas interface shape z_2 and the crystal radius are obtained by solving the Young-Laplace equation Eq. (6) under the following conditions.

$$2H = Boz_2 + \lambda \tag{6}$$

The boundary conditions are expressed as follows.

$$\theta = \theta_s \quad \text{at} \quad r = r_s \tag{7-1}$$

$$\theta = \theta_c \quad \text{at} \quad r = 1 \tag{7-2}$$

The melt volume is given by Eq. (8).

$$V_m = \int z_1 r dr + \int z_2 r dr \tag{8}$$

To solve the above problem, the Galerkin finite element method[3-5,8,11)] was used. Use of this method allows easy handling of the curved shapes of melt/crystal and melt/gas interfaces in comparison with the finite difference method.[1,2)] The present program incorporates isoparametric elements consisting of ninenoded quadrilateral as shown in **Fig. 2**.

In each finite element, temperature is approximated as follows.

$$T(r, z) = \sum \phi_i T_i \tag{9}$$

where ϕ_i is a biquadratic trial function.

The shape of the gas/melt interface is expressed by the following equation.

$$z_2 = \sum \psi_k z_{2k} \tag{10}$$

where ψ_k is a quadratic trial function.

By substituting Eqs. (9) and (10) into Eqs. (1)–(3) and (6), the Galerkin procedure gives a set of algebraic equations which was solved by an iterative Newton-Raphson scheme. To solve the matrix equations, the frontal solution technique by Hood[7] was used.

2. Results and Discussion

We compute the temperature fields in the melt and the silicon crystal rod of more than 12.5 cm in diameter. The physical properties and the processing parameters used in the numerical calculations are listed in **Table 1**,[4,11] where the temperature dependency of the thermal conductivity of crystal and the emissivity of crystal and radiation shield is taken into account.

Figures 3 and **4** show the effect of dimensionless pull rate *Pe* and crucible temperature T_c on the crystal radius and the melt/crystal interface shape without the radiation shield, where $\Delta z'$ is defined as the difference between z_1' and z_1' at $r' = r_s'$ as shown in Fig. 1. Apparently, the crystal radius decreases as *Pe* or T_c increases and the interface shape becomes less convex to crystal as *Pe* decreases. These results are in coincidence with the results of the previous workers.[3,11] It is concluded from the two figures that the interface becomes less convex by increasing crucible temperature and decreasing pull rate when the crystal radius is kept constant.

It is necessary to make the melt/crystal interface flatter in order to attain crystal perfection and homogeneous radial distribution of dopant, while, from the industrial point of view, single crystals must be pulled as fast as possible. Accordingly, the method based on the above conclusion is inadequate. Thus we examine the effect of a cylindrical radiation shield installed in the furnace as shown in Fig. 1.

Figure 5 shows the melt/crystal interface shapes for various values of radiation shield length l_{sh}, where *Pe* is constant but T_c changes in order to keep the crystal radius constant. The dotted line shows the interface shape without the radiation shield. It is found that inserting the radiation shield makes the melt/crystal interface less convex to the crystal in comparison with that without the shield, and that its effect becomes

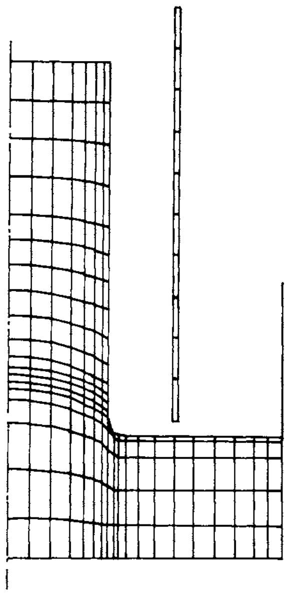

Fig. 2. Discretization of calculation domain for finite element method.

Table 1. Physical properties and processing parameter for silicon crystal growth

1. Physical properties
Melting point T_m': 1683 [K]
Latent heat of solidification ΔH_f: 1.8×10^6 [J/kg]
Thermal conductivity
melt k_l: 64 [W/m·K]
crystal k_s: $98.8924 - 9.4286595 \times 10^{-2} T + 2.889 \times 10^{-5} T^2$ [W/m·K]
radiation shield k_{sh}: 64 [W/m·K]
Density
melt ρ_l: 2420 [kg/m^3]
crystal ρ_s: 2300 [kg/m^3]
Heat capacity
melt C_{pl}: 1000 [J/kg·K]
crystal C_{ps}: 1000 [J/kg·K]
Emissivity
melt ε_l: 0.3
crystal ε_s: $0.9016 - 2.616 \times 10^{-4} T$; 0.64 if $T < 1000$ [K]
radiation shield ε_{sh}: $0.3789 + 2.015 \times 10^{-4} T$
crucible wall ε_c: 0.59
ambient wall ε_a: 0.8
Surface tension γ: 0.72 [N/m]
Contact angle
against crystal θ_s: 11 [deg]
against crucible θ_c: 90 [deg]
2. Processing parameter
Crucible radius r_c': 0.203 [m]
Crucible height z_c': 0.203 [m]
Crystal length l_s': 0.1624 [m] or 0.3654 [m]
Radiation shield length l_{sh}': 0.07105–0.3045 [m]
Radiation shield radius r_{sh}': 0.1218 [m]
Melt volume V_m': 0.016425 [m^3] or 0.012089 [m^3]
Ambient wall area A_a': 0.3884 [m^2]
Ambient wall temperature T_a': 673 [K]
Crucible temperature T_c': 1751–1856 [K]
Pull rate V_s': $4.167 \times 10^{-6} - 2.5 \times 10^{-5}$ [m/s]

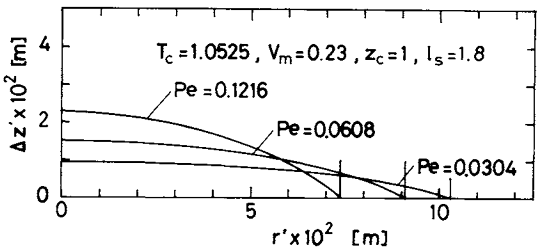

Fig. 3. Effect of *Pe* on crystal radius and melt/crystal interface shape.

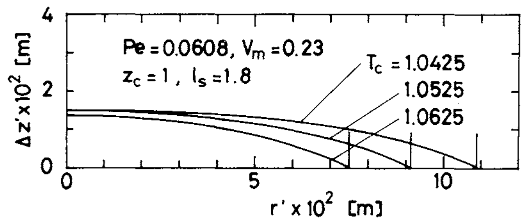

Fig. 4. Effect of crucible temperature on crystal radius and melt/crystal interface.

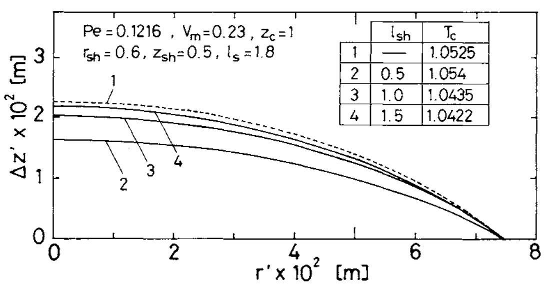

Fig. 5. Effect of radiation shield length on melt/crystal interface shape.

more remarkable as l_{sh} decreases. The isotherms in the melt, crystal and radiation shield for (a) no radiation shield and (b) $l_{sh}=0.5$ are given in **Fig. 6**.

Figure 7 shows the temperature distribution along the center line ($r=0$) and the crystal surface ($r=r_s$) for $l_{sh}=0$, 0.5 and 1.5. With the shorter radiation shield, the temperature gradient in the crystal, particularly near the melt/crystal interface, is steeper than that without the radiation shield because of reducing the radiated energy influx from the exposed hot crucible wall. It is found that with a short radiation shield ($l_{sh}=0.5$), the radial temperature difference near the interface becomes smaller than that without the radiation shield and also the axial temperature gradients at $r=0$ and $r=r_s$ become almost the same, providing a flatter interface shape. With the longer radiation shield, the temperature gradient near the interface is almost the same as that without the shield, but is less steep far from the interface. These results suggest that the radiation shield provides the possibility of a higher pull rate for a given interface shape or a flatter interface shape for a given pull rate. The larger thermal gradient, however, may produce larger thermal stress in the crystal. The smaller radial temperature difference may reduce the generation of dislocations caused by the thermal stress. The effect of the steeper lateral temperature gradient on the thermal stress should be further examined.

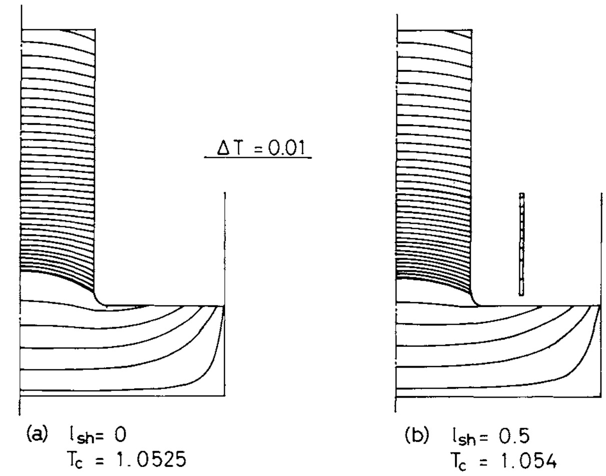

Fig. 6. Isotherms in melt and crystal.

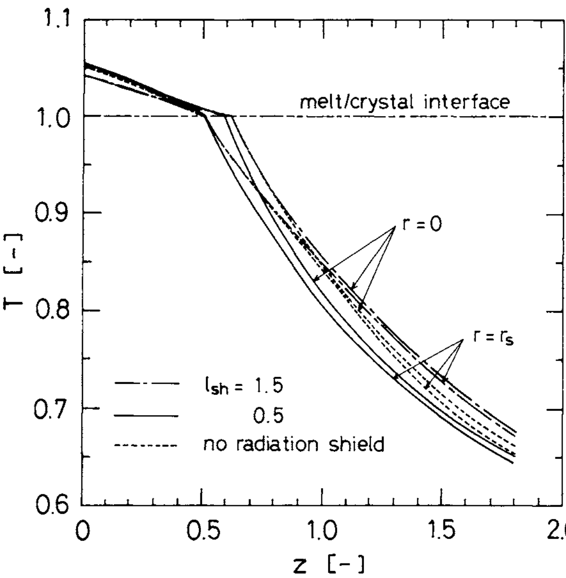

Fig. 7. Axial temperature distribution in melt and crystal.

In general, in order to keep the crystal diameter constant during crystal growth it is necessary to change the pull rate or crucible temperature. Thus knowledge of the response of the crystal radius to both the pull rate and the crucible temperature are required. **Figures 8** and **9** show the effect of pull rate and crucible temperature on the crystal radius in the presence of a radiation shield. Apparently, the crystal radius decreases as the pull rate or the crucible temperature increases, and both the gradients, particularly for $l_{sh}=0.5$, are less steep than those without radiation shield. It is found that by inserting the radiation shield the control of crystal diameter becomes easier.

Figure 10 shows how the melt/crystal interface

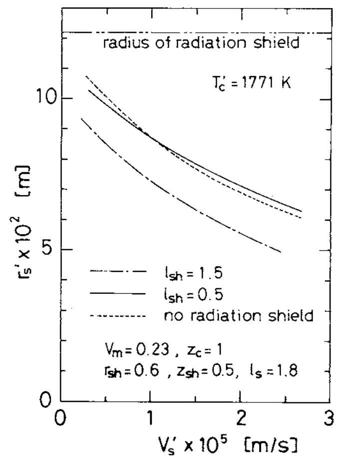

Fig. 8. Effect of pull rate on crystal radius.

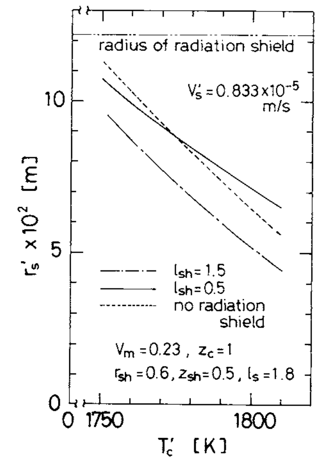

Fig. 9. Effect of crucible temperature on crystal radius.

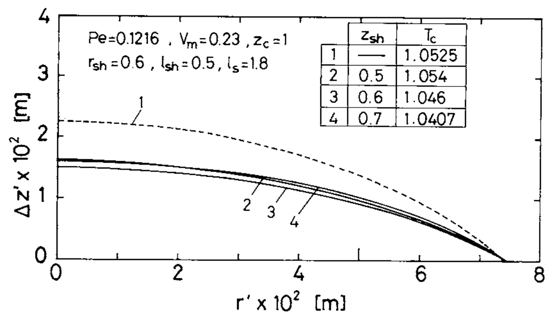

Fig. 10. Effect of radiation shield position on melt/crystal interface shape.

shape varies with the radiation shield position, that is, the distance z_{sh} between the crucible bottom and the lower end of the radiation shield. Apparently there exists an optimum position which makes the interface flattest.

Figure 11 shows the effect of emissivity of the radiation shield on the melt/crystal interface shape, where the shield length is 0.5. It is seen that as emissivity decreases the crucible temperature must be raised to keep the crystal radius constant and at the same time the interface becomes slightly less convex

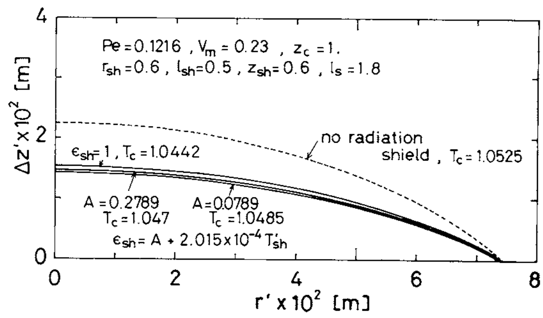

Fig. 11. Effect of emissivity of radiation shield on melt/crystal interface shape.

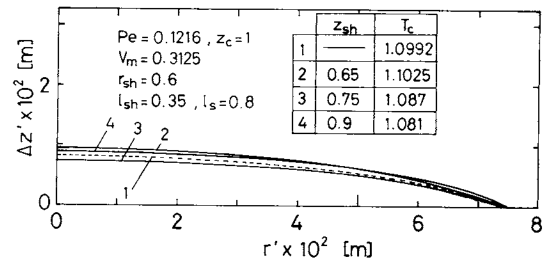

Fig. 12. Effect of radiation shield on melt/crystal interface shape at initial stage.

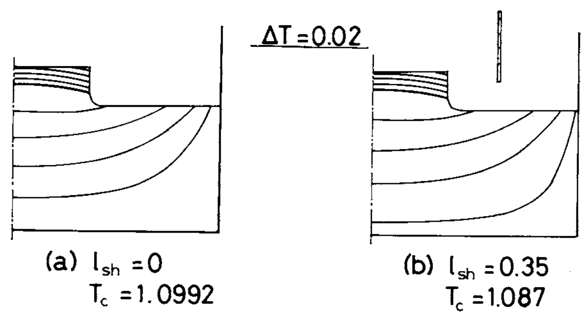

Fig. 13. Isotherms in melt and crystal at initial stage.

to the crystal.

So far we have discussed only the case with longer crystal rod. However, **Fig. 12** shows the effect of the radiation shield at the initial stage where the crucible height is higher than the crystal top surface, and the calculated temperature fields are shown in **Fig. 13**. Apparently, inserting the radiation shield into the furnace makes the interface shape more convex to the crystal than is true without the shield, except for $z_{sh} = 0.75$. Although there is an optimum position of the radiation shield similar to that in Fig. 10, the radiation shield has little effect on the flattening of the interface at the initial stage of growth.

Conclusion

For the silicon CZ system, the effect of inserting a radiation shield into the furnace on the temperature distribution in the melt and crystal and on the melt/crystal interface shape was studied theoretically and the following conclusions were obtained.

(1) A radiation shield makes the interface shape less convex to the crystal except at the initial stage.

(2) With a short radiation shield, there is a possibility of higher pull rate by increasing the temperature gradient near the melt/crystal interface.

Acknowledgment

This work was supported by Grant-in-Aid for Scientific Research (No. 61550696) from the Ministry of Education, Science and Calture of Japan. The numerical calculations were carried out by use of ACOS 1000 of the Computer Center of Tohoku Univ.

Nomenclature

A_k'	=	area of surface element	[m²]
A_k	=	$A_k'/2\pi r_c'^2$	[—]
Bo	=	Bond number $(=\rho_l r_c'^2\ g/\gamma)$	[—]
C_{ps}	=	heat capacity	[J/kg·K]
F_{jk}	=	Configuration factor	[—]
G_{jk}	=	Gebhart's absorption factor	[—]
g	=	gravitational acceleration	[m/s²]
H'	=	mean curvature	[1/m]
H	=	$r_c'H'$	[—]
ΔH_f	=	latent heat of solidification	[J/kg]
k	=	thermal conductivity	[W/m·K]
l_s'	=	crystal length	[m]
l_{sh}'	=	radiation shield length	[m]
l_s, l_{sh}	=	$l_s'/r_c', l_{sh}'/r_c'$	[—]
$\boldsymbol{n}$	=	outward-pointing normal at the boundary	[—]
Pe	=	Peclet number $(=\rho_s C_{ps} V_s' r_c'/k_l)$	[—]
p_G'	=	pressure in gas phase	[Pa]
p_0'	=	pressure at reference position	[Pa]
q_{rad}'	=	heat flux due to radiation	[J/m²·s]
q_{rad}	=	$q_{rad}' r_c'/k \cdot T_m'$	[—]
R_l	=	Radiation number $(=\varepsilon_l \sigma r_c' T_m'^3/k_l)$	[—]
r'	=	radial distance in cylindrical coordinates	[m]
r_c'	=	crucible radius	[m]
r_s'	=	crystal radius	[m]
r_{sh}'	=	radiation shield radius	[m]
r, r_s, r_{sh}	=	$r'/r_c', r_s'/r_c', r_{sh}'/r_c'$	[—]
St	=	Stefan number $(=\Delta H_f/C_{ps} \cdot T_m')$	[—]
T'	=	temperature	[K]
T_a'	=	ambient temperature	[K]
T_c'	=	crucible temperature	[K]
T_m'	=	melting-point temperature	[K]
T, T_a, T_c	=	$T'/T_m', T_a'/T_m', T_c'/T_m'$	[—]
$\Delta T'$	=	interval of isotherms	[K]
ΔT	=	$\Delta T'/T_m'$	[—]
V_m'	=	melt volume	[m³]
V_m	=	$V_m'/2\pi r_c'^3$	[—]
V_s'	=	crystal pull rate	[m/s]
z'	=	axial distance in cylindrical coordinates	[m]
z_c'	=	crucible height	[m]
z_{sh}'	=	distance between crucible bottom and lower end of radiation shield	[m]
z, z_c, z_{sh}	=	$z'/r_c', z_c'/r_c', z_{sh}'/r_c'$	[—]
z_1'	=	distance between crucible bottom and melt/crystal interface	[m]
z_2'	=	distance between crucible bottom and melt/gas interface	[m]
z_1, z_2	=	$z_1'/r_c', z_2'/r_c'$	[—]
$\Delta z'$	=	$z_1' - z_1'(r' = r_s')$	[m]
γ	=	surface tension	[N/m]
ε	=	emissivity	[—]
θ_c, θ_s	=	contact angle	[deg]
κ	=	ratio of thermal conductivity	[—]
λ	=	$(p_0' - p_G')r_c'/\gamma$	[—]
ρ	=	density	[kg/m³]
σ	=	Stefan-Boltzman constant	[W/m²·K⁴]
ϕ, ψ	=	trial function	[—]

⟨Subscripts⟩

l	=	melt
s	=	crystal
sh	=	radiation shield

Literature Cited

1) Arizumi, T. and N. Kobayashi: *Japan. J. Appl. Phys.*, **8**, 1091 (1969).
2) Arizumi, T. and N. Kobayashi: *J. Crystal Growth*, **13/14**, 615 (1972).
3) Derby, J. J., R. A. Brown, F. T. Geyling, A. S. Jordan and G. A. Nikolakopoulou: *J. Electrochem. Soc.*, **132**, 470 (1985).
4) Derby, J. J. and R. A. Brown: *J. Crystal Growth*, **74**, 605 (1986).
5) Derby, J. J. and R. A. Brown: *J. Crystal Growth*, **75**, 227 (1986).
6) van der Hart, A., and W. Uelhoff: *J. Crystal Growth*, **51**, 251 (1981).
7) Hood, P.: *Int. J. Num. Meth. Eng.*, **10**, 379 (1976).
8) Ramachandran, P. A. and M. P. Dudukovic: *J. Crystal Growth*, **71**, 399 (1985).
9) Rea, S. N.: *J. Crystal Growth*, **54**, 267 (1981).
10) Siegal, R. and J. R. Howell: Thermal Radiation Heat Transfer, McGraw-Hill, New York (1982).
11) Srivastava, R. K., P. A. Ramachandran and M. P. Dudukovic: *J. Crystal Growth*, **73**, 487 (1985).
12) Williams, G. and W. E. Renaser: *J. Crystal Growth*, **64**, 448 (1983).